Archosauromorphs (Reptilia: Diapsida) from the Lamy Quarry, Garita Creek Formation (Adamanian, Late Triassic), New Mexico, USA

Authors: Hégron, Axel, Stocker, Michelle R., Marsh, Adam D., and Nesbitt, Sterling J.

Source: Palaeodiversity, 13(1) : 135-149

Published By: Stuttgart State Museum of Natural History

URL: https://doi.org/10.18476/pale.v13.a11

Palaeodiversity 13: 135–149; Stuttgart 30 December 2020. Published online: 20 November 2020, DOI: 10.18476/pale.v13.a11

Archosauromorphs (Reptilia: Diapsida) from the Lamy Quarry, Garita Creek Formation (Adamanian, Late Triassic), New Mexico, USA

Axel Hégron, Michelle R. Stocker, Adam D. Marsh & Sterling J. Nesbitt

Abstract

The Lamy Quarry (= the Gunter bonebed) is known for its extensive accumulation of temnospondyl skulls and skeletons from the Norian (Upper Triassic) Garita Creek Formation, south of Lamy, New Mexico. Although the quarry is monodominant for metoposaurids, reptile fossils are also present. The reptile material, briefly described and identified to least-inclusive taxonomic levels, consists of several diagnostic elements from azendohsaurid and tanystropheid archosauromorphs based on apomorphies observed in the fossils. The most remarkable materials are two anterior cervical vertebrae and the posterior portion of a hemimandible that are identified as belonging to a *Malerisaurus*-like taxon within the Azendohsauridae. The vertebrae are two times longer than the holotype material of *Malerisaurus robinsonae* Chatterjee, 1980 and *Malerisaurus langstoni* Chatterjee, 1986, which suggests that azendohsaurids in the Late Triassic of North America reached much larger sizes than previously documented. The presence of a tanystropheid and azendohsaurid together supports the Adamanian age of the Garita Creek Formation and shows that azendohsaurids were present in what is now New Mexico.

Keywords: Azendohsauridae, Late Triassic, Tanystropheidae, Lamy Quarry, New Mexico, Chinle Formation.

1. Introduction

The Lamy Quarry, located just south of the town of Lamy, in north-central New Mexico (Fig. 1), has been an important locality for understanding Late Triassic vertebrates from the western United States and has provided important taxonomic, faunal, and taphonomic information of a death assemblage in a single accumulation. The quarry largely contains a single species of temnospondyl (*Anaschisma browni*, previously referred to *Buettneria perfecta*; Hunt & Lucas 1995; Gee et al. 2019), which has provided a wealth of information about metoposaurid anatomy (Colbert & Imbrie 1956), variation within the population (Colbert & Imbrie 1956), and population structure (Rinehart et al. 2008). Moreover, the taphonomy of the quarry has been well documented. The initial interpretation of a drought-induced death assemblage occurred soon after the first excavations (first interpreted by Romer 1939), although subsequent excavations and interpretations now suggest that drought was not a taphonomic factor (Hunt & Lucas 1989, 1995; Zeigler et al. 2002; Lucas et al. 2010).

Even though the Lamy Quarry bonebed contains the abundant remains of a single species of metoposaurid temnospondyl and is classified as monodominant (Lucas et al. 2010), reptile macrofossils (Hunt & Lucas 1995; Lucas et al. 2010) and microfossils of smaller vertebrates (Rinehart et al. 2001; Lucas et al. 2010) have been reported. The smaller vertebrates include a procoelous reptile caudal vertebra (Lucas et al. 2010), fish scales and skull elements of semionotids and redfieldiids (Rinehart et al. 2001; Lucas et al. 2010), and skull elements of small temnospondyls (Rinehart et al. 2001; Lucas et al. 2010). Among larger reptiles, an archosaur sacrum (Lucas et al. 2010) and isolated phytosaur teeth (Rinehart et al. 2001; Lucas et al. 2010) were recently identified, but other reptile remains were found during the original excavation by Harvard in the 1930s. This material was provisionally identified as an ‘unidentified reptile cervical’ (Hunt & Lucas 1995: fig. 2f, g), ‘unidentified reptile vertebra’ (Hunt & Lucas 1995: fig. 2b, c), ‘theropod ungual’ (Hunt & Lucas 1995: fig. 2e), and a ‘theropod caudal vertebra’ (Hunt & Lucas 1995: fig. 2d). With the exception of ‘unidentified reptile vertebra’ (Hunt & Lucas 1995: fig. 2b, c), we relocated this material in the Harvard collections and found additional reptile remains from the original excavation. Here, we reidentify and fully describe the reptile remains from the Lamy Quarry and compare them to similarly-aged reptiles across the western United States and India.

Abbreviations: FMNH, Field Museum of Natural History, Chicago, Illinois, U.S.A.; GR, Ruth Hall Museum of Paleontology, Ghost Ranch, New Mexico, U.S.A.; ISIR, Indian Statistical Institute, Kolkata, India; MCSN, Museo Civico di Storia Naturale di Milano, Milan, Italy; MCSNB, Museo Civico di Storia Naturale Enrico Caffi, Bergamo, Italy; MCZ, Museum of Comparative Zoology, Cambridge, Massachusetts, U.S.A.; NMMNH, New Mexico Museum of Natural History and Science, Albuquerque, New Mexico, U.S.A.; NSM, Nova Scotia Museum, Halifax, Nova Scotia, Canada; PEFO, Petrified Forest National Park, Arizona, U.S.A.; PIN, Paleontological Institute of the Russian Academy of Sciences, Moscow, Russia; SAM, Iziko

South African Museum, Cape Town, South Africa; TMM, Texas Vertebrate Paleontology Collections, The University of Texas at Austin, Austin, Texas, U.S.A.; UA, Université d'Antannanarivo, Antannanarivo, Madagascar; UCMP, University of California Museum of Paleontology, Berkeley, California, U.S.A.; UMMP, University of Michigan Museum of Paleontology, Ann Arbor, Michigan, U.S.A.

2. Material and methods

The fossils were prepared in the Fossil Preparation Laboratory at Virginia Tech. Broken fragments were adhered with Paraloid B-72, and an additional more dilute coat of Paraloid B-72 was used to preserve surfaces. Matrix was removed using a Micro Jack 1 (Paleotools.com), and acetone and water were used to remove the last bit of matrix with a toothbrush. Measurements were taken using a Pittsburgh 6" digital caliper. Centrum length was measured from the anterior and posterior ends of the preserved centrum. Centrum articular surface height was taken as a dorsoventral measurement from the outer rims of the anterior and/or posterior centrum articular surfaces. Centrum width was measured at the midline of the posterior articular surface facet from the outer rims. Neural spine length was measured between the dorsal ends of the neural spine, whereas neural spine height was taken dorsoventrally at the midline. Offset between articular facets was measured between the center of the anterior and posterior centrum articular facets.

3. Geologic setting and stratigraphy

The Lamy Quarry (=Gunter bonebed in Olsen, 1951, Hunt & Lucas 1995, Zeigler et al. 2002; Lamy amphibian Quarry) is located stratigraphically low in the Garita Creek Formation approximately 4 m above the underlying Tres Lagunas Member of the Santa Rosa Formation (Fig. 1; Hunt & Lucas 1995; Lucas et al. 2010). The quarry is associated with a distal floodplain facies (Lucas et al. 2010). The bonebed is ~10 cm thick and is composed of red sandy mudstones with green and purple mottles. These mudstones are interpreted as floodplain deposits that show evidence of pedogenic modification (e.g. colored mottles, carbonate nodules, and arthropod burrows) to form a calcific alfisol (Lucas et al. 2010), and this bonebed shows no signs of lacustrine deposition or severe drought as interpreted by Romer (1939).

4. Taphonomic comments

The bones do not possess traces of abrasion and are in an excellent state of preservation (Lucas et al. 2010), whereas realized bone damage is a consequence of sediment loading and unloading associated with the swelling and shrinkage of clays (Lucas et al. 2010). Almost all bones are disarticulated, and a preferred alignment is present that indicates hydraulic transport by a strong current along a short distance (Lucas et al. 2010). The bonebed has a high bone density and suggests a single brief depositional event (Lucas et al. 2010). Subaerial weathering is not observed on the bones (stage 0 of Behrensmeyer 1978), suggesting rapid burial. No damage due to trampling is observed, but some distortions on the surface of the fos-

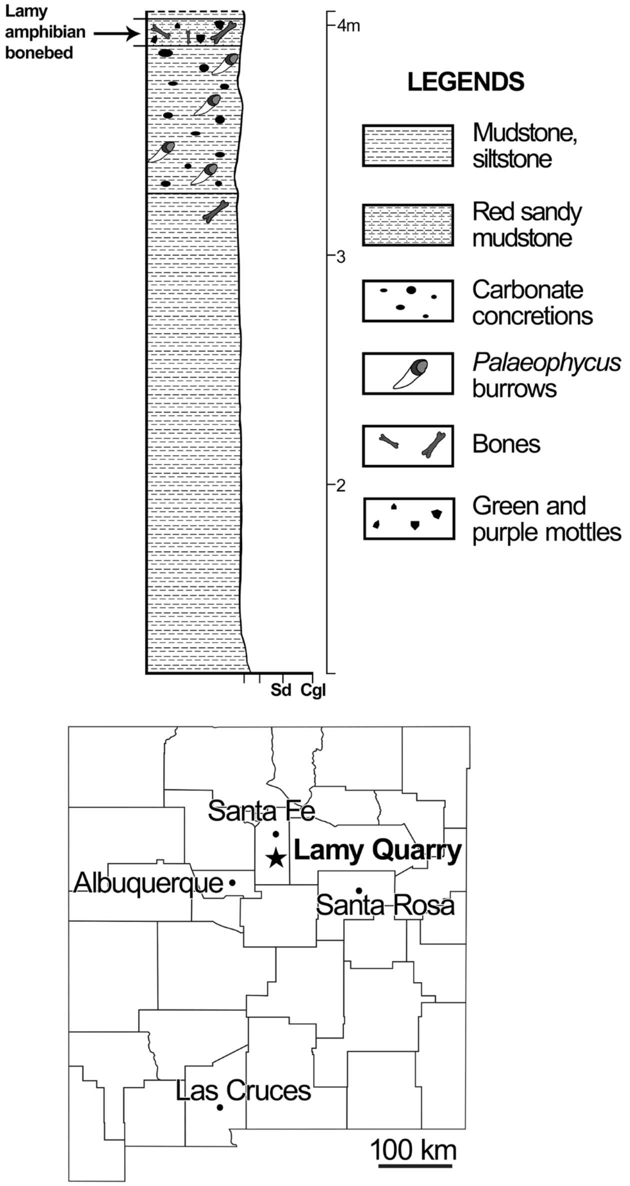

Fig. 1. Lithostratigraphic column of the Lamy Quarry (NMMNH L-1176, black star on New Mexico map beneath). Scale: thickness above Tres Lagunas Member (in m). Based on Lucas et al. (2010) and Martz et al. (2013).

sils due to bone wall collapse can be seen (Lucas et al. 2010). One likely cause of the formation of this bonebed is an aggregation associated with breeding populations (Rinehart et al. 2008).

The reptile cervical vertebrae (MCZ VPRA-9559 and MCZ 101539) described here have a similar preservation style compared to the metoposaurids in the bonebed (Lucas et al. 2010); they are crushed in and the surfaces are cracked, but the overall surface details are well-preserved and show little abrasion. The association of the reptile remains described here with each other or among the many disarticulated skeletons of metoposaurids was not recorded during collection and initial preparation. It appears that when reptile bones were identified, they were put together into a single box and then curated together. However, some association may have existed and was not recognized. For example, the remains of the azendohsaurid are about the same size and could have been from the same individual (see below).

5. Systematic palaeontology

Archosauromorpha v. Huene, 1946 (sensu Benton 1985)

Allokotosauria Nesbitt et al., 2015

Azendohsauridae Nesbitt et al., 2015

Referred material: MCZ VPRA-9559, anterior cervical vertebra; MCZ 101539, anterior cervical vertebra and rib fragment; MCZ 101531, conjoined articular and surangular; MCZ 101532, ungual; MCZ 101533, caudal vertebra; MCZ 101534, caudal vertebra; MCZ 101535, caudal vertebra; MCZ 101536, metatarsal II; MCZ 101577, broken neural spine.

Locality: NMMNH L-1176 in the Lamy Quarry (= Gunter bonebed), south of Santa Fe, near Lamy, New Mexico, USA (Romer, 1939). This locality is stratigraphically low in the Garita Creek Formation (Hunt & Lucas 1995; Lucas et al. 2010).

Age: Late Triassic (Norian), ?Adamanian holochronozone (Zeigler et al. 2002; Lucas et al. 2010). Based on lithostratigraphic and biostratigraphic correlations with other Dockum Group units, the Lamy Quarry is most likely early to middle Norian in age (Martz et al. 2013), instead of late Carnian (contra Zeigler et al. 2002; Lucas et al. 2010).

6. Descriptions

6.1. Lower jaw

MCZ 101531 (Fig. 2) consists of a posterior portion of a left hemimandible, with a nearly complete articular, broken retroarticular process, and the posterior portion of the surangular (see measurements in Table 4). The surangular is broken anteriorly and on its ventral edge, whereas the articular is well-preserved and only missing the posteromedial portion of the retroarticular process.

The surangular is co-ossified laterally to the articular, and no suture is visible; the fusion of the articular with surangular is found in many squamates such as in the Autarchoglossa (Conrad 2008) or Iguanidae (Cope 1892) and in rhynchocephalians such as *Diphydontosaurus avoni* (Whiteside 1986) and *Clevosaurus bairdi* (Sues et al., 1994). In the lateral view, the surangular is nearly flat, and there is no prominent lateral shelf preserved lateral to the articular. The ventral edge is straight, extends ventral of the articular, and is angled anteroventrally, and the ventral-most margin of the element curves slightly medioventrally, similar to that of *Trilophosaurus buettneri* (TMM 31025-140).

The articular possesses a well-preserved articulation surface with the quadrate in dorsal view. The articular facet (=glenoid) is complex; a convex ridge trending posterolaterally divides a posteromedial basin from an anterolateral slope (Fig. 2). A largely convex glenoid surface with a deep posteromedial basin is exclusively found in azendohsaurids, exemplified by *Azendohsaurus madagaskarensis* (Flynn et al. 2010), and a deep depression is

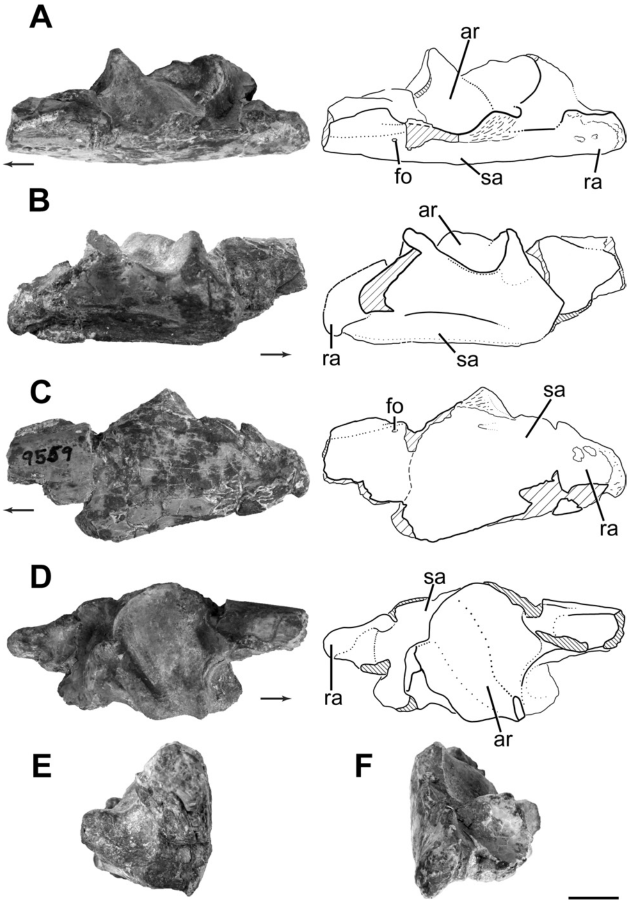

Fig. 2. Part of the posterior portions of the postdentary bones of the left hemimandible of an azendohsaurid, MCZ 101531; **A**: dorsolateral view; **B**: medial view; **C**: ventrolateral view; **D**: dorsal view; **E**: anterior view; **F**: posterior view. – Scale equals 1 cm. Arrows indicate the anterior direction. Cross-hatched areas indicated eroded or damaged surfaces. Abbreviations: ar, articular; fo, foramen; ra, retroarticular process; sa, surangular.

also present in *Malerisaurus langstoni* (TMM 31099-11) although this area is damaged. Laterally, the glenoid reaches the lateral surface of the surangular, but it is not clear if the surangular participates in the glenoid. Medially, the glenoid extends beyond the body of the rest of the articular, and a slight ridge demarcates the medial to posteromedial extent of the articulation surface. Just anterior to the medial extent of the glenoid, the articular surface rises to a peak extending dorsal to the glenoid surface and in line with the convex ridge trending posterolaterally from the glenoid. Anteriorly, the glenoid terminates on a small upturned ridge at a constricted anteriorly tapering portion of the articular. A tall ridge forms the posterior surface of the glenoid, and it is the tallest ridge of the articular. A trough is present at the peak of this ridge, and this trough extends medially. Just posterior to the peak, there is a small dorsally-open foramen anterolateral to the glenoid fossa on the lateral surface of the surangular, as in *Trilophosaurus buettneri* (TMM 31025-140). This is a potential synapomorphy of Allokotosauria (Nesbitt et al. 2015) and plesiomorphic for Archosauriformes (Ezcurra 2016). A posterior surangular foramen is also observed in extant reptiles (*Emoia loyaltiensis*; Daza et al., 2015, fig 7D; *Pseudogonatodes barbouri*, MCZ R-14385; Bauer et al. 2018).

Posterior to the articulation with the quadrate, the articular possesses a clear retroarticular process. There is no large dorsal expansion at the posterior end (=upturned process) as in other archosauromorphs (Ezcurra 2016). The length of the retroarticular process is moderate for an early diverging archosauromorph; the process is not as short as in *Azendohsaurus madagaskarensis* (Flynn et al. 2010) but not nearly as long as that of *Trilophosaurus buettneri* (TMM 31025-140), similar in length to the retroarticular process of *Malerisaurus robinsonae* (ISIR 150). The lateral edge of the retroarticular process bears a rounded process closer to the posterior edge of the glenoid than the posterior edge of the process. The posterior extent of the retroarticular process slightly expands laterally (contrary to *Malerisaurus robinsonae* where it extends mesially) into a rugose knob, and in lateral view the posterior end is gently rounded. The medial surface of the retroarticular process is broken, but it appears to have a dorsoventrally flattened process like that of *Trilophosaurus buettneri* (TMM 31025-140).

We identify MCZ 101531 as an azendohsaurid based on the morphology of the complex articulation surface between the articular and the quadrate. Known azendohsaurids, including MCZ 101531, possess a convex articular surface with a deep posteromedial depression that matches with a corresponding ventral end of the quadrate (Flynn et al. 2010; Nesbitt et al. 2015). Additionally, the retroarticular process appears to be anteroposteriorly short (character state 283:1, Ezcurra 2016) as in other azendohsaurids like *Malerisaurus robinsonae* (ISIR 150), *Malerisaurus langstoni* (TMM 31099-11), and *Pamelaria dolichotrachela* (Ezcurra 2016: fig. 29a), but not as short as in *Azendohsaurus madagaskarensis* (FMNH PR 2751).

6.2. Cervical vertebrae

Two similarly-sized anterior cervical vertebrae are preserved as disarticulated elements (MCZ VPRA-9559 and MCZ 101539), but it is not clear if they are from the same individual (MCZ VPRA-99 shows an offset of ~2.5° between its centrum articular facets whereas MCZ 101539 displays an offset of ~5°). MCZ VPRA-9559 (Fig. 3) has a broken anterior articular facet of the centrum, and the left prezygapophysis is missing.

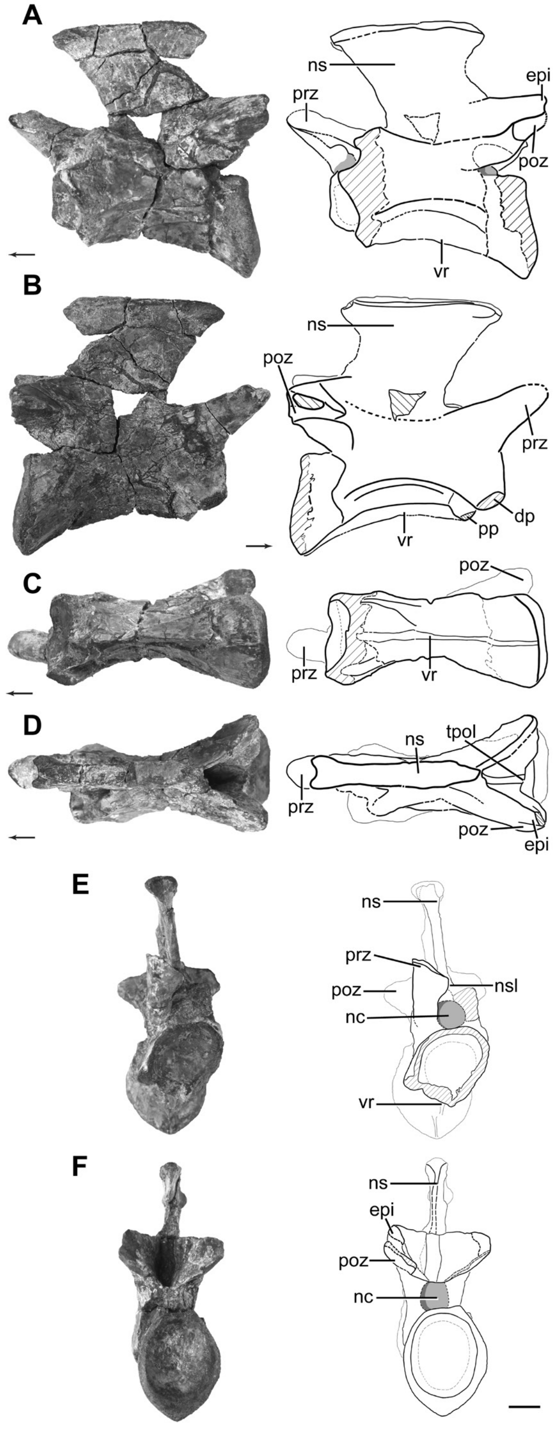

Fig. 3. Anterior cervical vertebra, MCZ VPRA-9959, of an azendohsaurid; **A**: left lateral view; **B**: right lateral view; **C**: ventral view; **D**: dorsal view; **E**: anterior view; **F**: posterior view. – Scale equals 1 cm. Arrows indicate the anterior direction. Cross-hatched areas indicated eroded or damaged surfaces. Abbreviations: dp, diapophysis; epi, epipophysis; nc, neural canal; ns, neural spine; nsl, neural spine lamina; poz, postzygapophysis; pp, parapophysis; prz, prezygapophysis; st, spine table; tpol, intrapostzygapophyseal lamina; vr, ventral ridge.

A small part of the neural arch ventral to the base of the neural spine is also absent. MCZ 101539 (Fig. 4) is missing the right postzygapophysis and has a broken anterior articular surface of the centrum. Based on morphological characters described below, we identify these vertebrae as anterior to mid cervicals (~ 3rd to 5th) based on similarities with *Azendohsaurus madagaskarensis* (Nesbitt et al. 2015) and other archosauromorphs (Ezcurra 2016).

The vertebrae are subequal in length (Table 1). The amphicoelous centra are about two and a half times as long anteroposteriorly as they are high dorsoventrally, as well as about two and a half times as long anteroposteriorly as wide mediolaterally (Table 2). Unfortunately, both anterior articular facets of the two vertebrae are slightly broken so the exact length of the centrum cannot be recorded; it is estimated to be around 70 mm based on the curvature of the preserved portion. The centra would be about three times as long anteroposteriorly as high dorsoventrally, which would be similar to those proportions of *Protorosaurus speneri* (Gottmann-Quesada & Sander 2009: text-fig. 12) and *Trilophosaurus buettneri* (TMM 31025-140; Spielmann et al. 2008). Both centra possess a ventral ridge at the midline that extends from the anterior to the posterior rims of the articular facets of the centrum. The ventral ridge is more pronounced in MCZ VPRA-9959, whereas parts of the ridge are broken in MCZ 101539. A ventral ridge at the midline is commonly shared by most early archosauromorphs (e.g., Gow 1975; Gottmann-Quesada & Sander 2009; Pritchard et al. 2015). The anterior and posterior articular surfaces of the centrum are oval and concave. There is a clear lip ventral to the posterior articular surface of MCZ VPRA-9959, whereas it is less developed in MCZ 101539. In lateral view, the cervical centra are parallelogram-shaped, where the anterior articular facets are elevated dorsally compared to the posterior facets; this is common in archosauromorphs with elongated cervical vertebrae (Gregory 1945; Sennikov 2005; Nesbitt et al. 2015; Ezcurra 2016). This configuration indicates that the head and neck were raised relative to the trunk and the neck was curved, which is a common occurrence in early archosauromorphs (Ezcurra 2016), as suggested for prolacertiforms (e.g. *Prolacerta broomi*; Gow 1975), azendohsaurids (e.g., *Azendohsaurus madagaskarensis*; Nesbitt et al. 2015) or tanystropheids (e.g., *Macrocnemus bassanii*; Jiang et al. 2011). The centra are co-ossified with the neural arches, and the neurocentral sutures are not visible.

The lateral extensions of the diapophyses are broken except for the right lateral one of MCZ VPRA-9959. The diapophysis is situated on a laterally elongated process, well separated from the parapophysis (contrary to the condition in *Protorosaurus speneri,* where diapophyses and parapophyses are fused into the same process), as in the archosauromorph *Vritramimosaurus dzerzhinskii* (Sennikov 2005), azendohsaurids *Azendohsaurus madagaskarensis* (FMNH PR 2791; Nesbitt et al. 2015) and *Pamelaria dolichotrachela* (ISIR 316/6; Sen, 2003), but more laterally elongated than in the trilophosaurid *Spinosuchus caseanus* (UMMP 7507; Spielmann et al. 2009). The base of the diapophysis contacts the outer rim of the anterior surface of the centrum like in most archosauromorphs, whereas diapophyses in *Trilophosaurus buettneri* (TMM 31025-140.; Spielmann et al. 2008) extend from the neural arches. The orientation of the diapophyses suggests a ventrolateral orientation for connection with the cervical rib. The parapophysis is only visible in left lateral view for MCZ 101539. It lies ventral to the diapophysis and extends laterally near the ventral edge of the centrum. A laterally concave crescentic fossa indents the lateral surface of the centrum, originating between the diapophyses

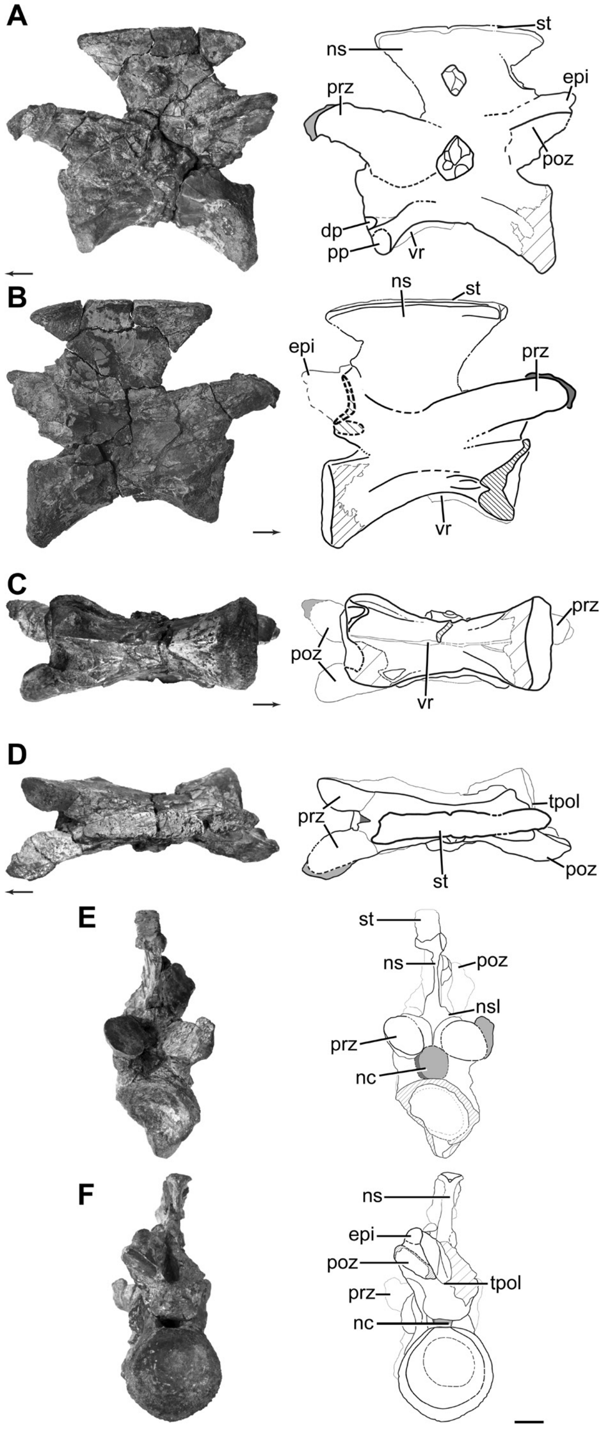

Fig. 4. Anterior cervical vertebra, MCZ 101539, of an azendohsaurid; **A**: left lateral view; **B**: right lateral view; **C**: ventral view; **D**: dorsal view; **E**: anterior view; **F**: posterior view. – Scale: 1 cm. Arrows indicate the anterior direction. Cross-hatched areas indicated eroded or damaged surfaces. Abbreviations: dp, diapophysis; epi, epipophysis; nc, neural canal; ns, neural spine; poz, postzygapophysis; pp, parapophysis; prz, prezygapophysis; st, spine table; tpol, intrapostzygapophyseal lamina; vr, ventral ridge.

and parapophyses and extending posteriorly to reach the midpoint of the centrum, but disappearing after that. A ridge extending from the posterior edge of the diapophysis dorsally frames the lateral fossa.

The cervical neural spines of these specimens are about twice as long anteroposteriorly as they are tall dorsoventrally, which is similar to *Prolacerta broomi* (UCMP 37151; Gow 1975), *Macrocnemus fuyuanensis* (MCSN V457; Jiang et al. 2011), *Langobardisaurus pandolfii* (MCSNB 2883; Renesto 1994), and *Azendohsaurus madagaskarensis* (UA 7-20-99-653; Nesbitt et al. 2015). The neural spines are also rectangular (dorsoventrally shorter than anteroposteriorly wide), as in tanystropheids, *Pamelaria dolichotrachela* (ISIR 316/1), and *Azendohsaurus madagaskarensis* (Nesbitt et al. 2015). Additionally, the dorsal edge of the neural spine has nearly the same length as its respective centrum, whereas the base of the neural spine is only half the length of the centrum; the base of the neural spine is located in the middle to posterior portion of the centrum. The neural spines are compressed transversally as thin blades as in *Prolacerta broomi* (UCMP 37151), *Trilophosaurus buettneri* (TMM 31025-140), and *Azendohsaurus madagaskarensis* (UA 7-20-99-653).

The dorsal margins of the neural spines expand laterally and are flattened dorsally forming a sub-rectangular 'spine table' that is mostly oriented horizontally to slightly slanted anterodorsally. Similar lateral expansions of the neural spine of the cervical vertebrae occur in *Malerisaurus robinsonae* (ISIR 150), *Vritramimosaurus dzerzhinskii* (PIN 951/72) and in a number of tanystropheids (Pritchard et al. 2015; Ezcurra 2016). The anterior end of the dorsal margin of the neural spines bifurcate at their termination. The two processes expand anteriorly, creating a notch between them at the midline and, consequently, the anterior end of the dorsal margin of the neural spine is wider than the rest of the neural spine. Posteriorly, the lateral margins of the dorsal surface of the neural spine converge to a point at the midline. It is possible that the anterior notch fits the posterior point in preceding and subsequent vertebrae. Both the anterior and posterior portions of the dorsal extent of the neural spine overhang the base of the neural spine as in the fourth cervical vertebra of *A. madagaskarensis* (UA 7-20-99-653; Nesbitt et al. 2015) and in aphanosaurs (Nesbitt et al. 2017a, 2017b).

The neural arches of the cervical vertebrae bear distinct prezygapophyses and postzygapophyses that extend laterally in lateral view; the articular facets of the prezygapophyses are angled dorsomedially around 30° to the horizontal. The articular facets of the postzygapophyses are angled ventrolaterally around 40° (Table 3). In the dorsal view, the prezygapophyses and postzygapophyses project about 30° laterally except for the remaining prezygapophyses of MCZ VPRA-9959, which shows a low angle of only 5° to the anteroposterior plane. However, the broken base of the other prezygapophysis projects about 30° also, which means the difference observed could be due to a taphonomic compression. The zygapophyses extend beyond the anterior and posterior articular surface of the centrum, respectively. The articular surfaces of the prezygapophyses are oval and dorsomedially oriented around 50° to the horizontal in MCZ 101539 and 40° to the horizontal in MCZ VPRA-9959 respectively. The postzygapophyses are ventrolaterally oriented around 35° to the horizontal in MCZ 101539 and around 30° in MCZ VPRA-9959. It is impossible to know the exact shape of the articular surfaces of the postzygapophyses as most of it are broken or missing. However, based on the remaining parts, it is plausible they were oval, as in a Late Triassic *Malerisaurus*-like taxon (PEFO 43981 and PEFO 43992) from the Dying Grounds (PFV 122), Petrified Forest National Park (Marsh et al. 2017). A nearly horizontal lamina (= intrapostzygapophyseal lamina) links the postzygapophyses across the midline, but the lamina is not horizontal and notched as in the trilophosaurids *Trilophosaurus buettneri* (TMM 31025-140) and *Spinosuchus caseanus* (UMMP 7507; Spielmann et al. 2009). The 'knob' on the lateral side of the prezygapophysis stalk found in *Azendohsaurus madagaskarensis* (UA 7-20-99-653; Nesbitt et al. 2015) is not present in MCZ VPRA-9959 and MCZ 101539.

The epipophysis is visible on the dorsal surface of the postzygapophysis of both vertebrae in left lateral view (Figs. 3, 4), and the epipophysis extends posterior to the articular surfaces of the postzygapophysis. Epipophyses also occur in early archosauromorphs like *Trilophosaurus buettneri* (TMM 31025-140), tanystropheids (Wild 1973; Pritchard et al. 2015), *Mesosuchus browni* (SAM-PK-588; Dilkes 1998), *Teraterpeton hrynewichorum* (NSM 999GF041; Sues 2003), *Vritramimosaurus dzerzhinskii* (Sennikov 2005), *Spinosuchus caseanus* (UMMP 7507; Spielmann et al. 2009), *Malerisaurus langstoni* (TMM 31099-11), and *Azendohsaurus madagaskarensis* (Nesbitt et al. 2015). In MCZ VPRA-9959 and MCZ 101539, hyposphene-hypantrum intervertebral articulations are clearly absent. In the anterior view, the neural spine bifurcates ventrally into thin laminae that terminate at the dorsal margin of the prezygapophyses (broken in MCZ 101539); these laminae and prezygapophyses frame an anterodorsally-oriented shallow fossa at the midline of the neural arch, floored by the roof of the neural canal, as in *Vritramimosaurus dzerzhinskii* (PIN 951/72). Posteriorly, the postzygapophyses diverge and frame a deep and narrow triangular depression at the midline in MCZ 101539 and MCZ VPRA-9959; this is also floored by the roof of the neural canal, similar to *Vritramimosaurus dzerzhinskii* (PIN 951/72). The anterior opening of the neural canal is visible in both vertebrae and is semicircular, whereas the posterior opening of MCZ VPRA-9959 is filled with matrix.

These vertebrae are identified as anterior to mid cervicals (~3rd – 5th) from an azendohsaurid based on the following combination of character states: they share an anteroposteriorly long and dorsoventrally low cervical neural spine (character 342:1 from Ezcurra 2016) found in *Pamelaria dolichotrachela* and *Azendohsaurus madagaskarensis* and the presence of a neural spine with an anterior overhang in the anterior cervical vertebrae (character 343:1 from Ezcurra 2016) with tanystropheids and the unnamed clade consisting of *Azendohsaurus madagaskarensis* + *Trilophosaurus buettneri*, parallelogram-shaped centrum of cervical vertebrae (character 313:1 from Ezcurra 2016) shared within Archosauromorpha, anterior margin of neural spine of the anterior postaxial cervical vertebrae inclined anterodorsally (character 116:1 from Nesbitt et al. 2015) as well as epipophyses present on the dorsal surface of postzygapophyses of the cervical vertebrae (character 119:1 from Nesbitt et al. 2015; character 336:1 from Ezcurra 2016) which are both present in allokotosaurs. The overall morphology of the Lamy cervicals is similar to those from *Malerisaurus* and *Vritramimosaurus dzerzhinskii* but the Lamy cervicals do not present ventromedial protrusions and the neural spine is not anteroposteriorly as long as the neural spine in *Vritramimosaurus dzerzhinskii*. The presence of a transversally expanded distal margin of the neural spine in the Lamy cervicals is shared with *Malerisaurus robinsonae* (ISIR 150) and in tanystropheids (e.g. GR269; Pritchard et al. 2015). Given its resemblance with cervical vertebrae from *Malerisaurus*, we tentatively identify these vertebrae as from a *Malerisaurus*-like taxon.

6.3. Caudal vertebrae

Three small disarticulated and broken caudal vertebrae were found in the quarry (MCZ 101533, MCZ 101534, MCZ 101535). MCZ 101533 (Fig. 5A–F) has broken prezygapophyses and postzygapophyses with only the base of the neural spine; both MCZ 101534 (Figure 5G–L) and MCZ 101535 (Fig. 5M–R) are badly damaged dorsally, missing an articular facet and both prezygapophyses and postzygapophyses.

MCZ 101533 is a slightly amphicoelous caudal vertebra with a centrum that is approximately three times longer anteroposteriorly than tall dorsoventrally and two and a half times longer anteroposteriorly than wide mediolaterally (Table 2). The centrum is compressed dorsoventrally. In the ventral view, two weak paramedian ridges extend to the articular facets and delimit a shallow groove as in *Azendohsaurus madagaskarensis* (Nesbitt et al. 2015) and *Trilophosaurus buettneri* (TMM 31025-140; Spielmann et al. 2008). No chevron facets are observed. The articular facets are sub-circular and have a ventral lip. In the lateral view, a ridge along the centrum linking the dorsal corners of the articular facets, delimits its lateral side and a suture is observed between the centrum and the neural canal. There are no transverse processes observed, and the ventral part of the vertebra is slightly convex in lateral view. The neural spine is broken in the distal part, very short anteroposteriorly, and located in the posterior part of the vertebra.

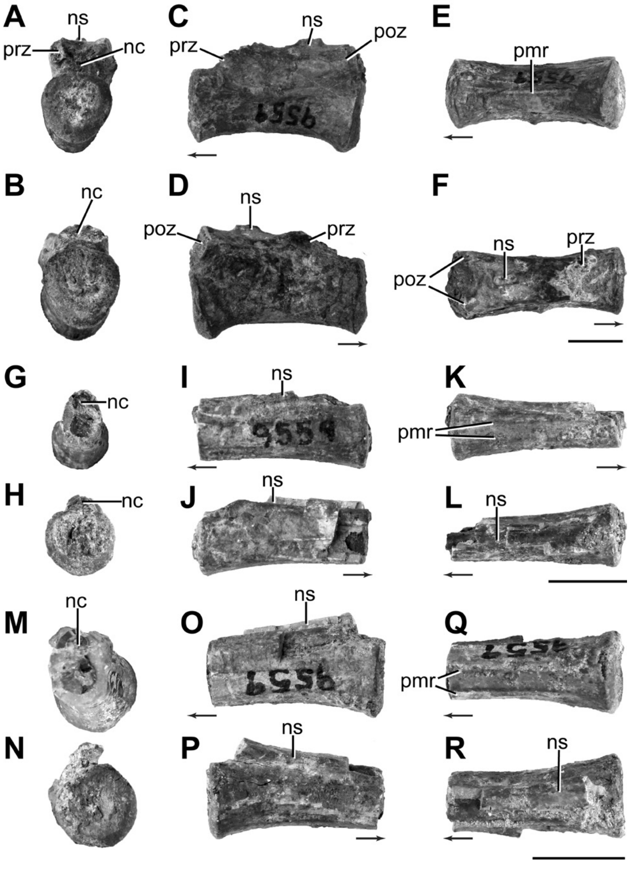

Fig. 5. Caudal vertebrae, MCZ 101533, of a possible azendohsaurid **A–F**; **A**: anterior view; **B**: posterior view; **C**: left lateral view; **D**: right lateral view; **E**: ventral view; **F**: dorsal view, Cervical vertebra MCZ 101534 **G–L;** **G**: anterior view; **H**: posterior view **I**: left lateral view; **J**: right lateral view; **K**: ventral view; **L**: dorsal view, Cervical vertebra MCZ 101535 **M–R**; **M**: anterior view; **N**: posterior view **O**: left lateral view; **P**: right lateral view; **Q**: ventral view; **R**: dorsal view. – Scale equals 5 mm. Arrows indicate the anterior direction. Abbreviations: nc, neural canal; ns, neural spine; pmr, paramedian ridge; poz, postzygapophysis; prz, prezygapophysis.

The anterior portions of the neural arches are completely broken, whereas only the bases of the postzygapophyses remain. The neural canal is filled with matrix. The general morphology, as well as the amphicoely and the presence of paramedian ridges delimiting a shallow groove, are also in MCZ 101534 and MCZ 101535 with only some slight differences. MCZ 101535 is only two times as long anteroposteriorly as high dorsoventrally, as well as two times longer anteroposteriorly than wide mediolaterally (Table 2), whereas MCZ 101534 possesses approximately the same ratios as MCZ 101533. MCZ 101534 and MCZ 101535 are broken dorsally and anteriorly, with circular articular surfaces. They both have an octagonal shape in anterior view at the cross-section of the broken anterior end and an octagonal-shaped posterior articular facet compared to MCZ 101533. In the same view, the neural canal is observed in both vertebrae and is circular. In the lateral view, two ridges approximately at mid-height along the centrum delimit the lateral side. The neural spine is absent in MCZ 101534, but a broken one is apparent in MCZ 101535; it is a flat, long, and low spine table that is slightly canted anteriorly in lateral view.

Given that the vertebrae are not well-preserved and that caudals do not have many diagnostic features, they are only identified as coming from reptiles. Amphicoely in the caudal vertebrae is shared in many early archosauromorphs (Gow 1975; Gottmann-Quesada & Sander 2009; Nesbitt et al. 2015). The paramedian ridges and the shallow groove are found in *Azendohsaurus madagaskarensis* (Nesbitt et al. 2015) and *Trilophosaurus buettneri* (Spielmann et al. 2008), as cited previously. The octagonal shape of the caudal vertebrae can also be observed in *Spinosuchus caseanus* (called *Trilophosaurus jacobsi* in Spielmann et al. 2008) and in the marine reptile clade Elasmosauridae (Otero et al. 2015; Lester 2019).

The morphology of the caudal vertebrae is consistent in form with that of *Azendohsaurus madagaskarensis*, but there are no clear synapomorphies linking them together. The size of each caudal vertebra is consistent with coming from the same individual and the size of the caudal vertebrae as a whole are consistent with the size of those of azendohsaurids (e.g., *Azendohsaurus madagaskarensis*).

6.4. Neural spine

A broken neural spine (MCZ 101577; Fig. 6) is nearly intact, only slightly broken in anterior and posterior view (see measurements in Table 4). It is not clear where in the vertebral column this neural spine would be located. The transversely compressed neural spine is rectangular in lateral view, with a dorsally rounded corner posteriorly (the anterior dorsal corner being broken). The dorsal margin of the neural spine is flattened into a 'spine table', horizontal in lateral view and slightly expanded transversally at the midline. The presence of a 'spine table' occurs in a variety of archosauromorphs and is thought

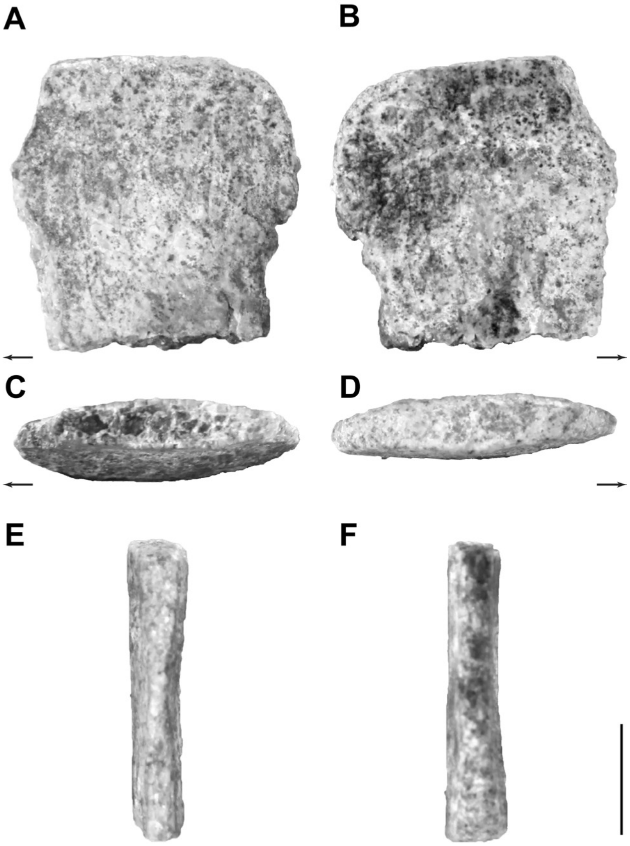

Fig. 6. Broken neural spine, MCZ 101577, of a possible azendohsaurid; **A**: left lateral view; **B**: right lateral view; **C**: ventral view; **D**: dorsal view; **E**: anterior view; **F**: posterior view. – Scale equals 5 mm. Arrows indicate the anterior direction.

to indicate well-developed musculature or to be associated with the presence of osteoderms (Patrick et al. 2019). In anterior and posterior views, the respective margins are rectangular. It resembles those on trunk vertebrae (19–25) of *Malerisaurus langstoni* (TMM 31099-11) from Chatterjee (1986), however, because there are no other distinctive features, it may have come from another archosauromorph.

6.5. Rib

A fragment of rib (Fig. 7) was found lying on top of one of the cervical vertebrae (MCZ 101539; see measurements in Table 4). In the anterior view, it has a distinct median groove as found in *Azendohsaurus madagaskarensis* (Nesbitt et al. 2015). In the lateral view, a small fossa is present near the anterior part of the rib. This partial rib is thin and has a weak lateral curvature, and it is sub-oval in cross-section. It may be a partial middle cervical rib from an azendohsaurid, because it was found with MCZ 101539.

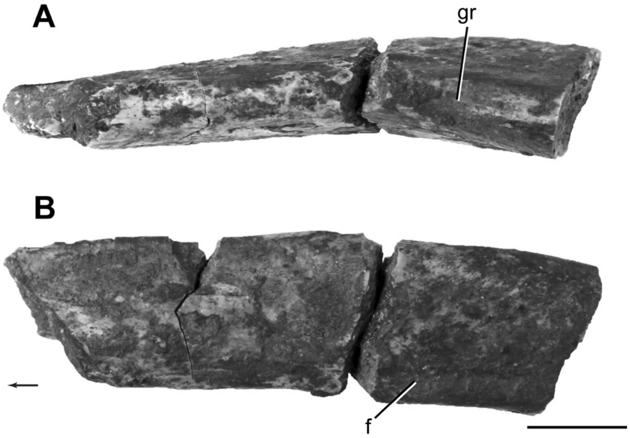

Fig. 7. Fragment of rib attached to cervical vertebra MCZ 101539 of an azendohsaurid; **A**: lateral view; **B**: anterior view. – Scale equals 1 cm. Arrow indicates the anterior direction. Abbreviations: f, fossa; gr, groove.

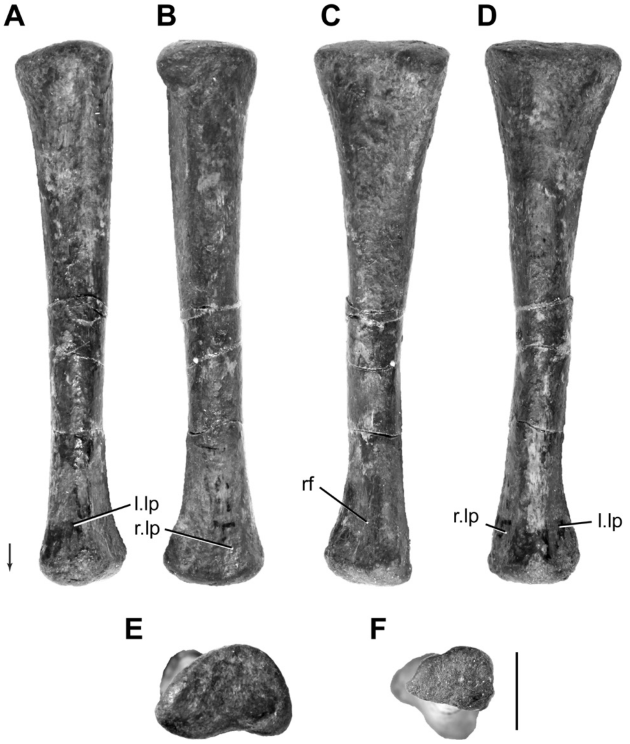

Fig. 8. Metatarsal II, MCZ 101536, of a possible azendohsaurid; **A**: left lateral view; **B**: right lateral view; **C**: ventral view; **D**: dorsal view; **E**: anterior view; **F**: posterior view. – Scale equals 5 mm. Arrow indicates the anterior direction. Abbreviations: l.lp, left ligament pit; rf, retractor fossa; r.lp, right ligament pit.

6.6. Metatarsal II

MCZ 101536 (Fig. 8) is a complete and well-preserved metatarsal II (see measurements in Table 4). The shaft is straight, with a slightly expanded proximal and distal end. The expansion is larger in the proximal part than the distal end. Both ends are slightly convex in left lateral view. It is remarkable for its length (52.7 mm); it is longer than the second metatarsal of *Azendohsaurus madagaskarensis* measuring approximately 44 mm (Nesbitt et al. 2015), although it is not as long as the longest metatarsal II from a *Malerisaurus*-like taxon (62 mm; PEFO 44168). In the proximal view, the articular surface appears sub-triangular with an apex corresponding to the midline of the shaft dorsally, different from the sub-rectangular articular end of metatarsal II in *Azendohsaurus madagaskarensis* (FMNH PR 2786; Nesbitt et al. 2015). MCZ 101536 is mediolaterally broader than dorsoventrally deep in proximal view. The proximal articular surface is slightly slanted medially, and a small fossa can be seen ventrally. The articular surfaces for the articulation with the proximal ends of other metatarsals are not distinct. The shaft is circular in cross-section at the midshaft similar to *Azendohsaurus madagaskarensis* (Nesbitt et al. 2015) but is more slender. In the distal view, the surface also is sub-triangular and slanted laterally. On each side there is a lateral ligament pit for the transverse metatarsal ligaments as in *Azendohsaurus madagaskarensis* (Nesbitt et al. 2015). A shallow retractor fossa proximal to the distal articular fossa is observed in ventral view, and a small and laterally slanted fossa is seen dorsally.

6.7. Ungual

MCZ 101532 (Fig. 9) is an anteroventrally-curved ungual with a broken tip (see measurements in Table 4). The ungual is mediolaterally-compressed, becoming thinner distally as in *Azendohsaurus madagaskarensis* (Nesbitt et al. 2015), *Malerisaurus robinsonae* (ISIR 150; Chatterjee 1980), and *Pamelaria dolichotrachela* (Sen 2003). MCZ 101532 possesses a concave proximal articular facet for articulation with the penultimate phalanx. In the lateral and medial views, a deep groove located ventrally separates the articular surface from a prominent tubercle on the ventral surface (=flexor process), as seen in *Azendohsaurus madagaskarensis* (UA 9-8-98-497; Nesbitt et al. 2015), *Trilophosaurus buettneri* (TMM 31025-140; Spielmann et al. 2008) and *Spinosuchus caseanus* (called *Trilophosaurus jacobsi* in Spielmann et al. 2008; Spielmann et al. 2009).

This ungual possesses a character state suggesting it was from an azendohsaurid: presence of a ventral tubercle well developed and extended ventral to the articular portion (character 233-1 from Nesbitt et al. 2015, also found as 587:1 from Ezcurra 2016) is shared with allokotosaurs and helps identify the ungual as a pedal ungual. Also, all known azendohsaurids share the same morphology of ungual: greatly compressed mediolaterally, curved, and with a sharp end (Chatterjee 1980; Sen 2003; Nesbitt et al. 2015).

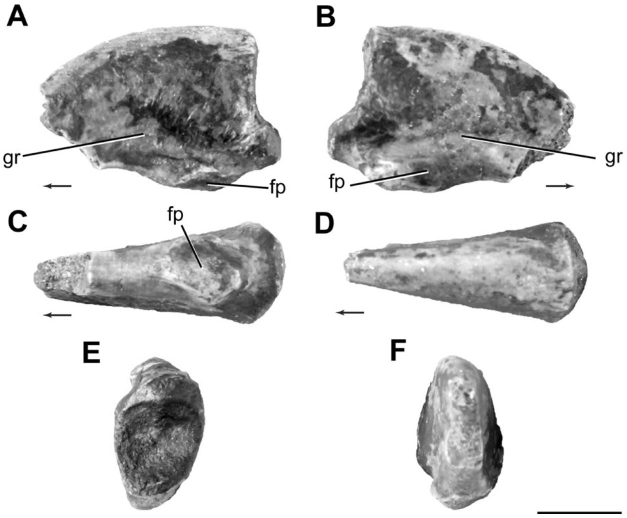

Fig. 9. Broken ungual, MCZ 101532, of an azendohsaurid; **A**: left lateral view; **B**: right lateral view; **C**: ventral view; **D**: dorsal view; **E**: anterior view; **F**: posterior view. – Scale equals 5 mm. Arrows indicate the anterior direction. Abbreviations: fp, flexor process; gr, groove.

Archosauromorpha v. Huene, 1946
(sensu Benton 1985)

Tanystropheidae Gervais, 1859

Referred material: MCZ 101537, caudal vertebra; MCZ 101538, anterior caudal vertebra.

Locality: NMMNH L-1176 in the Lamy Quarry (= the Gunter bonebed), south of Santa Fe, near Lamy, New Mexico, USA (Romer 1939). This locality is stratigraphically low in the Garita Creek Formation (Hunt & Lucas 1995; Lucas et al. 2010).

Age: Late Triassic (Norian), ?Adamanian holochronozone, early to middle Norian (see above; Zeigler et al. 2002; Lucas et al. 2010; Martz et al. 2013).

6.8. Caudal vertebrae

MCZ 101538 (Fig. 10A–F) is a small caudal vertebra with a right prezygapophysis and a broken right transverse process. The centrum is around two times longer anteroposteriorly than wide mediolaterally and around two times longer anteroposteriorly than tall dorsoventrally (Table 2), which is a smaller ratio compared to the approximately two and a half times longer-than-tall anterior caudal vertebrae from the Hayden Quarry (HQ) of Ghost Ranch (Pritchard et al. 2015). It shares similarities in morphology with anterior cervical vertebrae GR 357 and GR 281 from the HQ (Pritchard et al. 2015); the centrum is distinctly procoelous (= sub-circular, anteroventrally-inclined concave anterior facet and prominent convex, posterodorsally-inclined posterior condyle) as in *Langobardisaurus* and *Tanytrachelos* (Pritchard et al. 2015). There is a transversally-robust neural arch (only the right portion of the neural arch is present), the ventral surface of the centrum is rounded. In the right lateral view, a lamina connects the convex posterior facet with the base of a broken right transverse process located on the neural arch; it forms a crescentic, dorsally-convex and shallow fossa extending from the posterior articular facet to below the transverse process. The centrum is convex ventrally. In the ventral view, there is a ridge on the midline of the ventral surface extend-

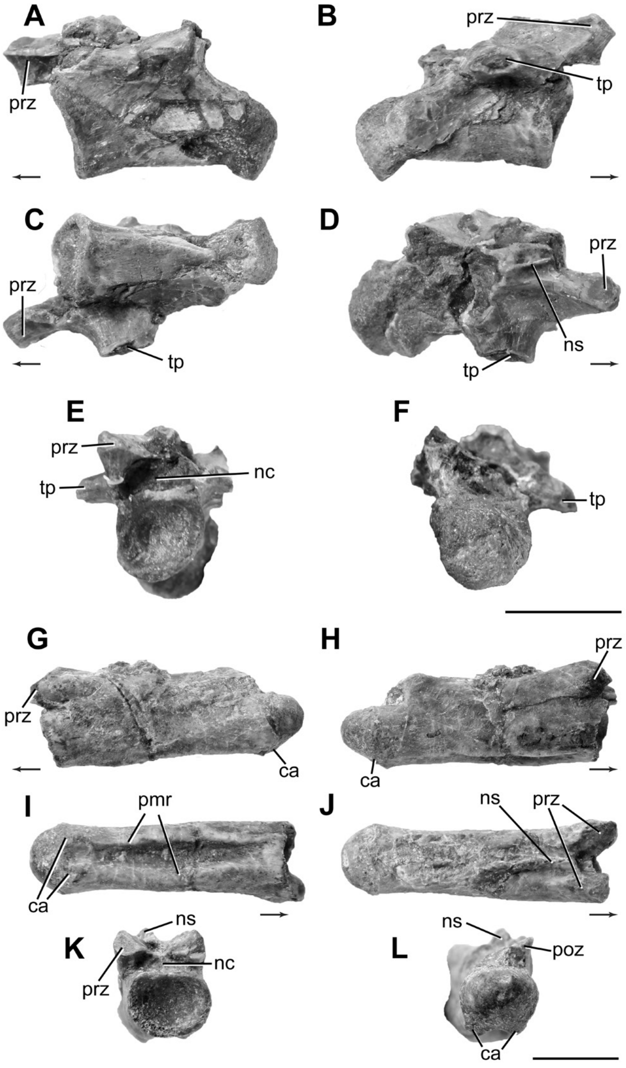

Fig. 10. Caudal vertebrae of a tanystropheid. Anterior caudal vertebra MCZ 101538 **A–F; A**: left lateral view; **B**: right lateral view; **C**: ventral view; **D**: dorsal view; **E**: anterior view; **F**: posterior view, Caudal vertebra MCZ 101537 **G–L**; **G**: left lateral view; **H**: right lateral view; **I**: ventral view; **J**: dorsal view; **K**: anterior view; **L**: posterior view. – Scale equals 5 mm. Arrows indicate the anterior direction. Abbreviations: ca, chevron articulation; nc, neural canal; ns, neural spine; pmr, paramedian ridges; prz, prezygapophysis; tp, transverse process.

ing between the articular facets of the centrum. Two small parasagittal expansions are observed on the ventral surface of the condyle. Small chevron facets are present on these expansions. In the dorsal view, the neural spine is broken; only the posterior part is present, but it was seemingly low and long. The right prezygapophysis originates from the neural arch; its articular facet is sub-oval and dorsomedially-oriented. On each side of the neural spine is found a deep fossa delimited laterally by the prezygapophyses. In the anterior view, only the right prezygapophysis is preserved; a triangular depression delimited by the neural arches and floored by the roof of the neural canal is present. The sub-circular neural canal is filled with matrix in anterior view and broken in posterior views.

MCZ 101537 (Fig. 10G–L) is a small vertebra with the remains of the right postzygapophyis and with broken prezygapophyses and neural spine. MCZ 101537 has a procoelous centrum (concave, anteroventrally-inclined anterior facet and convex posterior condyle), and this surface is approximately three times longer anteroposteriorly than wide mediolaterally, as well as three times longer anteroposteriorly than high dorsoventrally (Table 2). The vertebra is compressed dorsoventrally. The anterior articular facet is circular. In the right lateral view, a suture is observed between the neurocanal and the centrum, extending from the posterior articular facet to the mid-point of the vertebra. In the ventral view, a median groove extending to the articular facets is delimited on each side by a paramedian ridge and is similar to the morphology of *Langobardisaurus pandolfii* and *Tanystropheus longobardicus* (Pritchard et al. 2015). The paramedian ridges of MCZ 101537 originate from a small chevron facet distinct from the other, located on a small parasagittal expansion, also seen in *Langobardisaurus pandolfii* and *Tanystropheus longobardicus* (MCSN BES SC 265). In the dorsal view, the remain of a long and low neural spine is observed. The prezygapophyses originate from the neural arches and project laterally. The articular facets are oval and dorsomedially-oriented. On each side of the neural spine is found a fossa delimited laterally by the prezygapophyses. In the posterior view, the base of the right postzygapophysis is observed. The neural canal is only visible in anterior view and is circular.

The procoelous morphology of MCZ 101538 with a convex posterior condyle (character 102:2 from Pritchard et al. 2015) and morphology resembling anterior caudal vertebrae from the HQ suggest it is from a tanystropheid taxon similar to *Langobardisaurus pandolfii* and *Tanystropheus longobardicus*. For MCZ 101537, the transversely-compressed morphology, the presence of paramedian ridges and the presence of small chevron facets on the ventral surface indicates that this vertebra is a mid-to-posterior caudal. Procoely in tanystropheids is a synapomorphy of the clade *Langobardisaurus pandolfii* + *Tanytrachelos ahynis* in the phylogenetic analysis of Pritchard et al. (2015: character 102:2).

7. Discussion

7.1. Size of azendohsaurids in the Lamy Quarry

The centrum for each vertebra of the azendohsaurid in the Lamy Quarry is approximately two times anteroposteriorly longer than those of *Malerisaurus robinsonae* (ISIR 150; Chatterjee 1980) and *Malerisaurus langstoni* (TMM 31099-11; Chatterjee 1986), similar to the size range of other azendohsaurids such as *Azendohsaurus madagaskarensis* (Nesbitt et al. 2015), *Shringasaurus indicus* (Sengupta et al. 2017), and an unnamed *Malerisaurus*-like taxon from Petrified Forest National Park (Marsh et al. 2017; Nesbitt et al. 2017b). The anterior cervical vertebrae of the Lamy Quarry azendohsaurid are slightly anteroposteriorly longer than the fourth or fifth cervical vertebra from *Shringasaurus indicus* (Sengupta et al. 2017: table s2). The centrum in the cervical vertebrae of the Lamy Quarry azendohsaurid is also around two and a half times longer anteroposteriorly than wide mediolaterally; these proportions are similar to those found in previous studies on the species of *Malerisaurus* (Chatterjee 1980; Chatterjee 1986) where the centra were three times longer anteroposteriorly than mediolaterally wide, which shows that anterior cervical vertebrae kept approximately the same length to width ratio, even in longer cervicals. This could imply that both species of *Malerisaurus* are far from the maximum body size for the genus (or clade) given our inferred close relationship between the Lamy material and *Malerisaurus.*

The relationship between size and somatic maturity in *Malerisaurus* and azendohsaurids has yet to be studied in detail (but see Cubo & Jalil 2019), and the somatic maturity of the large *Malerisaurus*-like specimens from the Lamy Quarry is difficult to access. Unfortunately, no azendohsaurid femur was found in the Lamy Quarry so growth could not be assessed through traditional histological techniques or direct size comparison. The neurocentral sutures of MCZ VPRA-9559 and MCZ 101539 are closed, but the overall size and the closure of neurocentral sutures can be a poor indicator of skeletal maturity in the absence of growth lines in osteohistological data (Irmis 2007; Cubo & Jalil 2019; Griffin 2020).

7.2. Late Triassic archosauromorph diversity

Our identifications of an azendohsaurid and an additional occurrence of a tanystropheid at the Lamy Quarry demonstrates that these clades were more widespread in western Pangea than previously thought. Furthermore, both taxa are part of a larger, global realization, that early archosauromorphs had a much wider distribution across Pangea and were diverse. However, the presence of these archosauromorphs in Middle Triassic and Late Triassic terrestrial deposits around the world has been largely overlooked for two reasons. First, groups like azendohsaurids are closely related to relatively better-known archosauromorphs such as rhynchosaurs and trilophosaurids (Nesbitt et al. 2015; Ezcurra 2016), and the many plesiomorphies these groups share make azendohsaurids cryptic in their respective assemblages until autapomorphic remains are found. Second, allokotosaur remains have been unidentified or misidentified in their respective assemblages (e.g., *Malerisaurus robinsonae* tentatively identified as belonging to Protorosauridae, Chatterjee 1980; *Pamelaria dolichotrachela* first identified as a prolacertid, Sen 2003; *Spinosuchus caseanus* misidentified as the theropod dinosaur *Coelophysis* sp., Case 1922; partial pterygoids of an archosauromorph previously identified as specimens of the captorhinidae *Polystichodontos mandibularis* from the Otis Chalk localities, Elder 1978). This was because robust saurian phylogenetic hypotheses (Nesbitt et al. 2015; Ezcurra 2016; Pritchard & Nesbitt 2017) and new and more complete representative specimens (e.g., Flynn et al. 2010; Stocker 2013; Nesbitt et al. 2015; Sengupta et al. 2017) were not available until relatively recently, which made it impossible to utilize apomorphy-based identifications (Bell et al. 2010; Nesbitt & Stocker 2008; Martz et al. 2013; Stocker 2013; Lessner et al. 2018) for many groups of non-archosaur archosauromorphs. Careful identifications of these early archosauromorphs are key to realizing the complete evolutionary histories near the end of the radiation of the Triassic archosauromorphs.

8. Conclusions

Other than a massive death assemblage of metoposaurid temnospondyls, the Lamy Quarry also preserves rare, but diagnostic, reptile remains. From the quarry, we identify cranial and postcranial bones from an azendohsaurid allokotosaur and vertebrae from a tanystropheid. The azendohsaurid is notable for its large size compared to other Late Triassic members of the clade from the western United States. Furthermore, azendohsaurids were more widely distributed than previously thought, highlighting their diversification in western Pangaea. The presence of an azendohsaurid and a tanystropheid is consistent with other Adamanian-aged assemblages in Upper Triassic deposits of the western United States. The study and reinterpretation of unidentified or misinterpreted specimens from this quarry helps understand the diversification of archosauromorphs in the Late Triassic.

Acknowledgements

We thank Jessica Cundiff (MCZ) and Christina Byrd (MCZ) for curating the specimens and Stephanie Pierce (MCZ) for allowing the specimens to be loaned. Travis Oishi prepared the two cervical vertebrae and Vicki Yarborough helped prepare and curate the specimens. Thanks to Martín Ezcurra for providing photographs of *Malerisaurus robinsonae* for comparison. Adam Pritchard and an anonymous reviewer are greatly thanked for providing constructive reviews. This is Petrified Forest National Park Paleontological Contribution No. 76. The views presented herein are those of the authors and not necessarily those of the United States Government.

9. References

Bauer, A. M., Beach-Mehrotra, M., Bermudez, Y., Clark, G. E., Daza, J. D., Glynne, E. & Willett, J. (2018): The tiny skull of the Peruvian gecko *Pseudogonatodes barbouri* (Gekkota: Sphaerodactylidae) obtained via a divide-and-conquer approach to morphological data acquisition. – South American Journal of Herpetology, **13** (2): 102–116.

Behrensmeyer, A. K. (1978): Taphonomic and ecologic information from bone weathering. – Paleobiology, **4** (2): 150–162.

Bell, C. J., Gauthier, J. A. & Bever, G. S. (2010): Covert biases, circularity, and apomorphies: a critical look at the North American Quaternary Herpetofaunal Stability Hypothesis. – Quaternary International, **217**: 30–36.

Benton, M. J. (1985): Classification and phylogeny of the diapsid reptiles. – Zoological Journal of the Linnean Society, **84**: 97–164.

Case, E. C. (1922): New reptiles and stegocephalians from the Upper Triassic of western Texas. – Carnegie Institution of Washington Publication, **321**: 84 pp.

Chatterjee, S. (1980): *Malerisaurus*, a new eosuchian reptile from the Late Triassic of India. – Philosophical Transactions of the Royal Society of London, (B), **291**: 163–200.

Chatterjee, S. (1986): *Malerisaurus langstoni*, a new diapsid reptile from the Triassic of Texas. – Journal of Vertebrate Paleontology, **6**: 297–312.

Colbert, E. H. & Imbrie, J. (1956): Triassic metoposaurid amphibians. – Bulletin of the American Museum of Natural History, **110**: 399–452.

Conrad, J. L. (2008): Phylogeny and systematics of Squamata (Reptilia) based on morphology. – Bulletin of the American Museum of Natural History, **310**: 1–182.

Cope, E. D. (1892): The osteology of the Lacertilia. – Proceedings of the American Philosophical Society, **30** (138): 185–221.

Cubo, J. & Jalil, N.-E. (2019): Bone histology of *Azendohsaurus laaroussii*: implications for the evolution of thermometabolism in Archosauria. – Paleobiology, **45**: 317–330.

Daza, J. D., Bauer, A. M., Sand, C., Lilley, I., Wake, T. A. & Valentin, F. (2015): Reptile Remains from Tiga (Tokanod), Loyalty Islands, New Caledonia1. – Pacific Science, **69** (4): 531–557.

Dilkes, D. W. (1998): The early Triassic rhynchosaur *Mesosuchus browni* and the interrelationships of basal archosauromorph reptiles. – Philosophical Transactions of the Royal Society of London, (B), **353**: 501–541.

Elder, R. L. (1978): Paleontology and paleoecology of the Dockum Group, Upper Triassic, Howard County, Texas. – Unpublished MS thesis: 206 pp.; Austin (University of Texas).

Ezcurra, M. D. (2016): The phylogenetic relationships of basal archosauromorphs, with an emphasis on the systematics of proterosuchian archosauriforms. – PeerJ, **4**: e1778.

Flynn, J. J., Nesbitt, S. J., Parrish, M. J., Ranivoharimanana, L. & Wyss, A. R. (2010): A new species of *Azendohsaurus* (Diapsida: Archosauromorpha) from the Triassic Isalo Group of southwestern Madagascar: cranium and mandible. – Palaeontology, **53**: 669–688.

Gee, B. M., Parker, W. G. & Marsh, A. D. (2019): Redescription of *Anaschisma* (Temnospondyli: Metoposauridae) from the Late Triassic of Wyoming and the phylogeny of the Metoposauridae. – Journal of Systematic Palaeontology, **18**: 233–258.

Gervais, P. (1859): Zoologie et paléontologie françaises (2nd edition). 544 pp.; Paris (Bertrand).

Gottmann-Quesada, A. & Sander, P. M. (2009): A redescription of the early archosauromorph *Protorosaurus speneri* Meyer, 1832, and its phylogenetic relationships. – Palaeontographica, (A), **287**: 123–220.

Gow, C. E. (1975): The morphology and relationships of *Youngina capensis* Broom and *Prolacerta broomi* Parrington. – Palaeontologia Africana, **18**: 89–131.

Gregory, J. T. (1945): Osteology and relationships of *Trilophosaurus*. – University of Texas Publications, **4401**: 273–359.

Griffin, C. T. (2020): The influence of developmental patterns on vertebrate evolution, with the evolution of the sacrum and pelvis as a case study. – Ph.D. dissertation, Virginia Tech: 253 pp.; Blacksburg.

Huene, F. v. (1946): Die großen Stämme der Tetrapoden in den geologischen Zeiten. – Biologisches Zentralblatt, **65**: 268–275.

Hunt, A. P. & Lucas, S. G. (1989): Late Triassic vertebrate localities in New Mexico. – In: Hunt, A. P. & Lucas, S. G. (eds.): Dawn of the Age of Dinosaurs in the American Southwest: 72–101; Albuquerque (New Mexico Museum of Natural History).

Hunt, A. P. & Lucas, S. G. (1995): Vertebrate paleontology and biochronology of the lower Chinle Group (Upper Triassic) Santa Fe County, north–central New Mexico. – New Mexico Geological Society Guidebook, **46**: 243–246.

Irmis, R. B. (2007): Axial skeleton ontogeny in the Parasuchia (Archosauria: Pseudosuchia) and its implications for ontogenetic determinations in archosaurs. – Journal of Vertebrate Paleontology, **27**: 350–361.

Jiang, D.-Y., Rieppel, O., Fraser, N. C., Motani, R., Hao, W.-C., Tintori, A., Sun, Y.-L & Sun, Z.-Y. (2011): New information on the protorosaurian reptile *Macrocnemus fuyuanensis* Li et al. 2007, from the Middle/Upper Triassic of Yunnan, China. – Journal of Vertebrate Paleontology, **31**: 1230–1237.

Lessner, E. J., Parker, W. G., Marsh, A. D., Nesbitt, S. J., Irmis, R. B. & Mueller, B. D. (2018): New insights into Late Triassic dinosauromorph-bearing assemblages from Texas using apomorphy-based identifications. – PaleoBios, **35**: 1–41.

Lester, E. (2019): Description and histology of a small-bodied elasmosaur and description of *Mortuneria seyemourensis* postcranium. – M.S. thesis, Marshall University: 61 pp. https://mds.marshall.edu/etd/1210

Lucas, S. G., Rinehart, L. F., Krainer, K., Spielmann, J. A., & Heckert, A. B. (2010): Taphonomy of the Lamy amphibian quarry: A Late Triassic bonebed in New Mexico, U.S.A. – Palaeogeography, Palaeoclimatology, Palaeoecology, **298**: 388–398.

Marsh, A. D., Parker, W. G., Kligman, B. T. & Lessner, E. J. (2017): Bonebed of a carnivorous archosauromorph from the Chinle Formation (Late Triassic: Norian) of Petrified Forest National Park. – Geological Society of America Abstracts with Programs, **49**: 221-4.

Martz, J. W., Mueller, B., Nesbitt, S. J., Stocker, M. R., Parker, W. G., Atanassov, M., Fraser, N., Weinbaum, J. & Lehane, J. R. (2013): A taxonomic and biostratigraphic re-evaluation of the Post Quarry vertebrate assemblage from the Cooper Canyon Formation (Dockum Group, Upper Triassic) of southern Garza County, western Texas. – Earth and Environmental Science Transactions of the Royal Society of Edinburgh, **103**: 339–364.

Nesbitt, S. J. & Stocker, M. R. (2008): The vertebrate assemblage of the Late Triassic Canjilon Quarry (northern New Mexico, USA) and the importance of apomorphy-based assemblage comparisons. – Journal of Vertebrate Paleontology, **28**: 1063–1072.

Nesbitt, S. J., Butler, R. J., Ezcurra, M. D., Charig, A. J. & Barrett, P. M. (2017a): The anatomy of *Teleocrater rhadinus*, an early avemetatarsalian from the lower portion of the Lifua Member of the Manda Beds (Middle Triassic). – Journal of Vertebrate Paleontology Memoir, **17**: 142–177.

Nesbitt, S. J., Flynn, J. J., Pritchard, A. C., Parrish, J. M., Ranivoharimanana, L. & Wyss, A. R. (2015): Postcranial osteology of *Azendohsaurus madagaskarensis* (?Middle to Upper Triassic, Isalo Group, Madagascar) and its systematic position among stem archosaur reptiles. – Bulletin of the American Museum of Natural History, **398**: 1–126.

Nesbitt, S. J., Stocker, M. R., Ezcurra, M., Fraser, N. C., Heckert, A. B., Marsh, A. D., Parker, W. G., Mueller, B. & Pritchard, A. C. (2017b): The "strange reptiles" of the Triassic: the morphology, ecology, and taxonomic diversity of the clade Allokotosauria illuminated by the discovery of an early diverging member. – Journal of Vertebrate Paleontology, Program and Abstracts, **2017**: 168–169.

Olsen, R. (1951): Size relations in the limb bones of Buettneria perfecta. – Journal of Paleontology, **25**: 520–524.

Otero, R.A., Soto-Acuña, S., Salazar, C. & Oyarzún, J.L. (2015): New elasmosaurids (Sauropterygia, Plesiosauria) from the Late Cretaceous of the Magallanes Basin, Chilean Patagonia: Evidence of a faunal turnover during the Maastrichtian along the Weddellian Biogeographic Province. – Andean Geology, **42** (2): 237–267.

Patrick, E. L., Whiteside, D. I. & Benton, M. J. (2019): A new crurotarsan archosaur from the Late Triassic of South Wales. – Journal of Vertebrate Paleontology, **39** (3): e1645147.

Pritchard, A. C., Turner, A. H., Nesbitt, S. J., Irmis, R. B. & Smith, N. D. (2015): Late Triassic tanystropheids (Reptilia, Archosauromorpha) from northern New Mexico (Petrified Forest Member, Chinle Formation) and the biogeography, functional morphology, and evolution of Tanystropheidae. – Journal of Vertebrate Paleontology, **35**: e911186.

Pritchard, A. C. & Nesbitt, S. J. (2017): A bird-like skull in a Triassic diapsid reptile increases heterogeneity of the morphological and phylogenetic radiation of Diapsida. – Royal Society Open Science, **4**: 170499.

Renesto, S. (1994): A new prolacertiform reptile from the Late Triassic of Northern Italy. – Rivista Italiana di Paleontologia e Stratigrafia, **100**: 285–306.

Rinehart, L., Lucas, S. & Heckert, A. (2001): Microvertebrate fossils from the late Carnian Lamy amphibian quarry, east-central New Mexico. – New Mexico Geology, **23**: 64 pp.

Rinehart, L. F., Lucas, S. G., Heckert, A. B. & Hunt, A. P. (2008): Preliminary analysis of growth and age structure of *Buettneria* (Amphibia: Metoposauridae) assemblages from the Upper Triassic of West Texas and New Mexico. – New Mexico Geology, **30**: 56 pp.

Romer, A. S. (1939): An amphibian graveyard. – The Scientific Monthly, **49**: 337–339.

Sen, K. (2003): *Pamelaria dolichotrachela*, a new prolacertid reptile from the Middle Triassic of India. – Journal of Asian Earth Sciences, **21** (6): 663–681.

Sengupta, S., Ezcurra, M. D. & Bandyopadhyay, S. (2017): A new horned and long-necked herbivorous stem-archosaur from the Middle Triassic of India. – Scientific Reports, **7**: 8366.

Spielmann, J. A., Lucas, S. G., Rhinehart, L. F. & Heckert, A. B. (2008): The Late Triassic Archosauromorph *Trilophosaurus*. – New Mexico Museum of Natural History and Science Bulletin, **43**: 1–177.

Spielmann, J. A., Lucas, S. G., Heckert, A. B., Rinehart, L. F. & H.R. Richards (2009): Redescription of *Spinosuchus caseanus* (Archosauromorpha: Trilophosauridae) from the Upper Triassic of North America. – Palaeodiversity, **2**: 283–313.

Stocker, M. R. (2013): Contextualizing vertebrate faunal dynamics: New Perspectives from the Triassic and Eocene of western North America. – Ph.D. dissertation, the University of Texas at Austin: 297 pp.; Austin.

Sues, H. D., Shubin, N. H. & Olsen, P. E. (1994): A new sphenodontian (Lepidosauria: Rhynchocephalia) from the McCoy Brook Formation (Lower Jurassic) of Nova Scotia, Canada. – Journal of Vertebrate Paleontology, **14** (3): 327–340.

Sues, H.-D. (2003): An unusual new archosauromorph reptile from the Upper Triassic Wolfville Formation of Nova Scotia. – Canadian Journal of Earth Sciences, **40**: 635–649.

Whiteside, D. I. (1986): The head skeleton of the Rhaetian sphenodontid *Diphydontosaurus avonis* gen. et sp. nov. and the modernizing of a living fossil. – Philosophical Transactions of the Royal Society of London, (B), **312** (1156): 379–430.

Wild, R. (1973): Die Triasfauna der Tessiner Kalkalpen XXII. *Tanystropheus longobardicus* (Bassani). – Schweizerische Paläontologische Abhandlungen, **95**: 1–162.

Zeigler, K. E., Lucas, S. G. & Heckert, A. B. (2002): Taphonomy of the Late Triassic Lamy amphibian quarry (Garita Creek Formation: Chinle Group), central New Mexico. – New Mexico Museum of Natural History and Science Bulletin, **21**: 279–283.

Addresses of the authors

Axel Hégron, Univ. Rennes, CNRS, Géosciences Rennes – UMR 6118, 35000 Rennes France & Department of Geosciences, Virginia Tech, Blacksburg, VA 24061, USA; e-mail: axelhegron@gmail.com

Michelle R. Stocker, Sterling J. Nesbitt, Department of Geosciences, Virginia Tech, Blacksburg, VA 24061, USA; e-mail: stockerm@vt.edu, sjn2104@vt.edu

Adam D. Marsh, Petrified Forest National Park, 1 Park Road #2217, Petrified Forest, AZ 86028, USA; e-mail: adam_marsh@nps.gov

Manuscript received: 30 September 2020, revised version accepted: 14 October 2020.

Identification	Referred specimen	Element identified	Anterior centrum end height (mm)	Posterior centrum end height (mm)	Centrum width (mm)	Full centrum length (mm)	Neural spine length (mm)	Neural spine height (mm)
Azendohsauridae	MCZ 101539	Anterior cervical	23.97e	24.32	22.73	58.85e	47.91	24.16
Azendohsauridae	MCZ VPRA-9559	Anterior cervical	N/A	26.51	24.12	59.03e	43.03e	26.83
Azendohsauridae	MCZ 101533	Caudal vertebra	8.62	9.42	10.95	26.52	3.81e	N/A
Azendohsauridae	MCZ 101534	Caudal vertebra	N/A	7.55	8.52	21.65e	11.76e	1.28e
Azendohsauridae	MCZ 101535	Caudal vertebra	N/A	8.69	8.38	18.36e	11.11e	0.74e
Tanystropheidae	MCZ 101537	Anterior caudal vertebra	4.15	4.68	4.46	14.66	N/A	N/A
Tanystropheidae	MCZ 101538	Caudal vertebra	3.66	3.89	3.93	8.64	N/A	N/A

Table 1. Measurements of the azendohsaurid vertebrae and tanystropheid vertebrae. N/A indicates this portion was unable to be determined with the represented material, and "e" indicates an estimated value. Methods used to take the measures can be found in the Material & Method section.

Identification	Referred specimen	Element identified	Full centrum length/Anterior centrum end height	Full centrum length/Posterior centrum end height	Full centrum length/Centrum width	Neural spine length/Neural spine height
Azendohsauridae	MCZ 101539	Anterior cervical	2.33	2.42	2.46	1.98
Azendohsauridae	MCZ VPRA-9559	Anterior cervical	N/A	2.23	2.45	1.60
Azendohsauridae	MCZ 101533	Caudal vertebra	3.08	2.82	2.42	N/A
Azendohsauridae	MCZ 101534	Caudal vertebra	N/A	2.87	2.54	9.13
Azendohsauridae	MCZ 101535	Caudal vertebra	N/A	2.11	2.19	15.01
Tanystropheidae	MCZ 101537	Anterior caudal vertebra	3.53	3.13	3.29	N/A
Tanystropheidae	MCZ 101538	Caudal vertebra	2.22	2.36	2.20	N/A

Table 2. Different ratios based on the measurement of the azendohsaurid vertebrae and tanystropheid vertebrae. Methods used to take the measures can be found in the Material & Method section.

Referred specimen	Lateral inclination of prezygapophyses in left lateral view	Lateral inclination of postzygapophyses in left lateral view	Lateral inclination of prezygapophyses in dorsal view	Lateral inclination of postzygapophyses in dorsal view	Dorsomedial inclination of prezygapophyses	Ventrolateral inclination of postzygapophyses	Articular facets offset
MCZ 101539	25°	36°	32°	26°	50°	35°	5°
MCZ VPRA-9559	37°	40°	5°	36°	40°	30°	2.5°

Table 3. Prezygapophyses and postzygapophyses angle measurements of the *Malerisaurus*-like azendohsaurid anterior cervical vertebrae. Methods used to take the measures can be found in the Material & Method section.

Referred specimen	Element identified	Height (mm)	Length (mm)	Width (mm)	Proximal width (mm)	Distal width (mm)	Mid-shaft width (mm)
MCZ 101531	Left hemimandible	22.31	44.06	20.39			
MCZ 101577	Neural spine	13.54	13.3	1.87			
MCZ 101532	Ungual	9.42	13.97	5.52			
MCZ 101539	Rib	13.75	44.45	8.06			
MCZ 101536	Metatarsal II	10.82	52.7		13.23	9.39	5.95

Table 4. Measurement of an isolated neural spine and non-vertebrae azendohsaurid fossils found in the quarry. Methods used to take the measures can be found in the Material & Method section.